A theory crack healing in polymers

R. P. Wool and K. M. O'Connor

Related Articles

Strain rate sensitivity and activation volume of Cu/Ni metallic multilayer thin films measured via micropillar compression
Appl. Phys. Lett. 101, 051901 (2012)

Prediction of the propagation probability of individual cracks in brittle single crystal materials
Appl. Phys. Lett. 101, 041903 (2012)

Autonomic restoration of electrical conductivity using polymer-stabilized carbon nanotube and graphene microcapsules
Appl. Phys. Lett. 101, 043106 (2012)

Nano-scale fracture toughness and behavior of graphene/epoxy interface
J. Appl. Phys. 112, 023510 (2012)

Theoretical model of hardness anisotropy in brittle materials
J. Appl. Phys. 112, 023506 (2012)

Additional information on J. Appl. Phys.
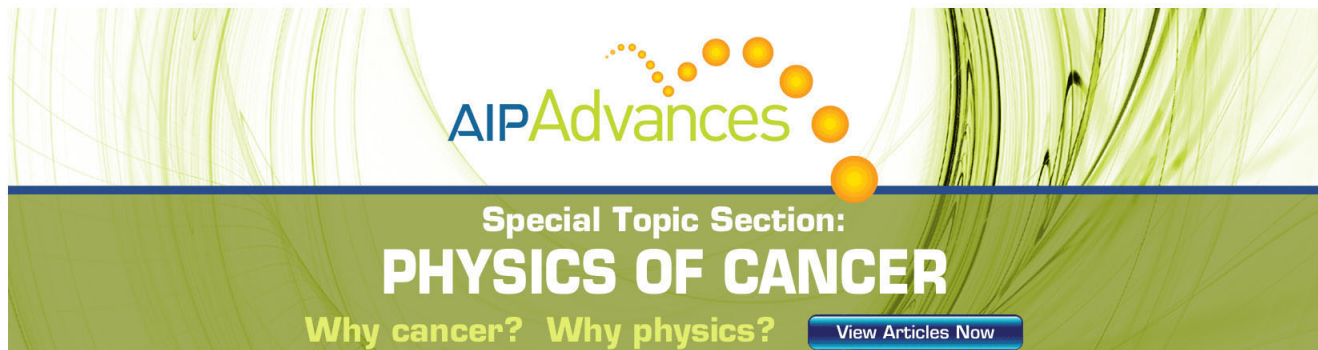
Journal Homepage: http://jap.aip.org/

Journal Information: http://jap.aip.org/about/about_the_journal

Top downloads: http://jap.aip.org/features/most_downloaded

Information for Authors: http://jap.aip.org/authors

A theory of crack healing in polymers

R. P. Wool and K. M. O'Connor

Department of Metallurgy and Mining Engineering, University of Illinois, Urbana, Illinois 61801

A theory of crack healing in polymers is presented in terms of the stages of crack healing, namely, (a) surface rearrangement, (b) surface approach, (c) wetting, (d) diffusion, and (e) randomization. The recovery ratio R of mechanical properties with time was determined as a convolution product, $R = R_h(t)*\phi(t)$, where $R_h(t)$ is an intrinsic healing function, and $\phi(t)$ is a wetting distribution function for the crack interface or plane in the material. The reptation model of a chain in a tube was used to describe self-diffusion of interpenetrating random coil chains which formed a basis for $R_h(t)$. Applications of the theory are described, including crack healing in amorphous polymers and melt processing of polymer resins by injection or compression molding. Relations are developed for fracture stress σ, strain ϵ, and energy E as a function of time t, temperature T, pressure P, and molecular weight M. Results include (i) during healing or processing at $t < t_\infty$, $\sigma, \epsilon \sim t^{1/4}$, $E \sim t^{1/2}$; (ii) at constant $t < t_\infty$, $\sigma, \epsilon \sim M^{-1/4}$, $E \sim M^{-1/2}$; (iii) in the fully interpenetrated healed state at $t = t_\infty$, $\sigma, \epsilon \sim M^{1/2}$, $E \sim M$; (iv) the time to achieve complete healing, $t_\infty \sim M^3$, $\sim \exp P$, $\sim \exp 1/T$. Chain fracture, creep, and stress relaxation are also discussed. New concepts for strength predictions are introduced.

PACS numbers: 81.40.Np, 62.20.Mk, 46.30.Nz

I. INTRODUCTION

The topic of crack healing in polymer materials has received considerable attention in the past few years.[1-17] Recent results indicate that while crack healing is an interesting concept in itself, it provides a new insight into understanding fundamental concepts of the strength of materials. In this paper, we provide a microscopic theory for healing in polymers in which mechanical properties, e. g., stress, strain, modulus, and impact energy, are related to time, temperature, pressure, molecular weight, and constitution of the material. Examination of mechanical property restoration during healing permits one to converge on the optimal properties of the virgin state in terms of the aforementioned variables. Thus, the crack healing theory prescribed herein has extensive application to materials where cracks, crazes, and voids are not obviously involved in mechanical property control. This point is very clearly demonstrated in this paper in terms of mechanical property predictions for polymers as a function of processing time, temperature, and pressure.

II. THE EXPERIMENTAL CONCEPT

The experimental concept for crack healing is a simple one and is portrayed in Fig. 1. Here, we consider a polymer in the virgin state at some reference condition with known mechanical properties, such as fracture stress σ_∞, elongation to break ϵ_∞, tensile modulus Y_∞, impact energy or fracture energy E_∞, and general spectroscopic measures I_∞ of molecular or microstructural parameters via infrared, NMR, light scattering, x ray, etc. The material is then taken to some damaged state possibly involving cracks, crazes, voids, or incipient voids via a reference deformation history. The damaged material is subjected to a healing history involving healing time t_h, healing temperature T_h, and healing pressure P_h. The (partially) healed material properties σ, ϵ, Y, E, and I are then examined and compared with that of the virgin state via convenient dimensionless recovery ratios R as

$$R(\sigma) = \sigma/\sigma_\infty, \tag{1a}$$

$$R(\epsilon) = \epsilon/\epsilon_\infty, \tag{1b}$$

$$R(E) = E/E_\infty, \tag{1c}$$

$$R(I) = I/I_\infty, \tag{1d}$$

where $0 \leqslant R \leqslant 1$.

The ratio R compares a property of the healed state with that of the virgin state with respect to t_h, T_h, and P_h. Thus, experimentally we obtain the function

$$R = R(t_h, T_h, P_h) \tag{2}$$

for a particular material, with reference to both the virgin state and to the damage state. The major consideration in this paper is to develop an understanding of the healing function on a microscopic level.
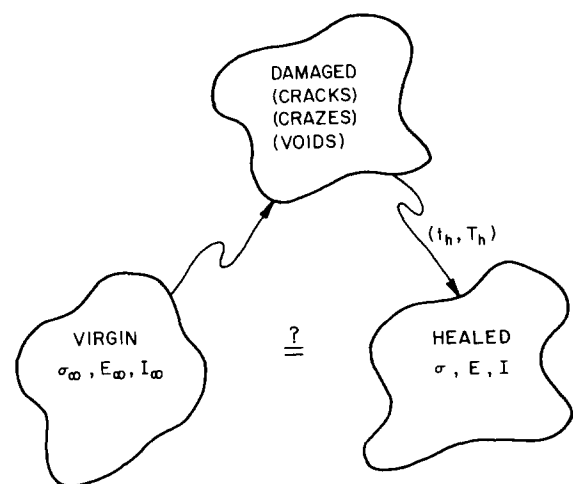

FIG. 1. Experimental approach to healing in polymers is shown. A virgin material is damaged and then healed. The healed material is compared with the virgin material via mechanical or spectroscopic measures as a function of healing time t_h and temperature T_h.

III. GENERAL OBSERVATIONS

Healing experiments have been conducted on most categories of polymeric materials, including semicrystalline polymers, amorphous glassy polymers, block copolymers, filled and unfilled elastomers, and fiber reinforced composites.[1–9,12,13] Experimental methods included stress-strain measurements at constant strain rate, stress relaxation at constant strain, creep at constant load, sinusoidal fatigue stress, Izod impact, double cantilever beam, and peel force experiments. These mechanical deformation histories were applied to the reference material configuration at room temperature and atmospheric pressure. Healing was conducted at atmospheric pressure or in vacuum, for healing times t_h ranging from 0 minutes to years (in some cases), and at healing temperatures T_h from $T_g - 50$ °C to $T_g + 100$ °C, where T_g is the glass transition temperature.

With increasing t_h at constant T_h, we observe the following:

Fracture stress	$\sigma \rightarrow \sigma_\infty$,
Fracture energy	$E \rightarrow E_\infty$,
Elongation to break	$\epsilon \rightarrow \epsilon_\infty$,
Fatigue life	$N_f \rightarrow \infty$,
Mullins effect	Disappears,
Stress relaxation modulus	$G(t) \rightarrow G_\infty(t)$,
Creep compliance	$J(t) \rightarrow J_\infty(t)$.

(3)

In cases where microscopy, spectroscopy, or scattering experiments confirm their presence, cracks, crazes, and microvoids are observed to disappear and heal concurrently with the restoration of mechanical properties listed in Eq. (3). Cracks can heal by line mode (uniform healing at all points in the crack interface), by point mode (healing at the crack tip only), or by mixed modes.[3] For crazes, the nucleation time $\tau \rightarrow \infty$ and the growth rate $g \rightarrow 0$, with increasing t_h at constant T_h.[9]

An empirical kinetic theory of healing[2,3] is useful for determining recovery with time, such that at constant T_h,

$$R \simeq 1 - \frac{1 - R_0}{(1 + Kt_h)^\alpha},$$

(4)

in which R_0, K, and α are constants. Equation (4), while predicting the general sigmoidal behavior observed for healing processes with an appropriate time-temperature superposition of healing data at different T_h, is, nonetheless, strictly empirical and without microscopic physical foundation. However, certain solutions to crack healing problems determined by the new microscopic theory will have formulations similar to Eq. (4).

A. Effect of T_h on R

At constant t_h for healing temperatures T_1 and T_2, we generally have

$$R(T_1) \geqslant R(T_2),$$

(5)

if $T_1 > T_2$. The $>$ sign applies for $T_1 > T_2 \geqslant T_g$ and the $=$ sign applies for T_1 and $T_2 \ll T_g$. The temperature dependence can be included in Eq. (4) by an empirical Arrhenius form for the constant K, as

$$K = K_0 e^{-E_a/kT}$$

(6)

in which K_0, E_a, and k are a constant, an activation energy, and the Boltzmann constant, respectively. The microscopic theory will demonstrate how temperature controls the healing rate from three different aspects and for most cases Eq. (6) will not be strictly valid, but remains of some empirical importance.

IV. THEORETICAL CONSIDERATIONS
A. Stages of healing

The recognition of the different sequential stages of crack healing is essential to the formulation of a microscopic
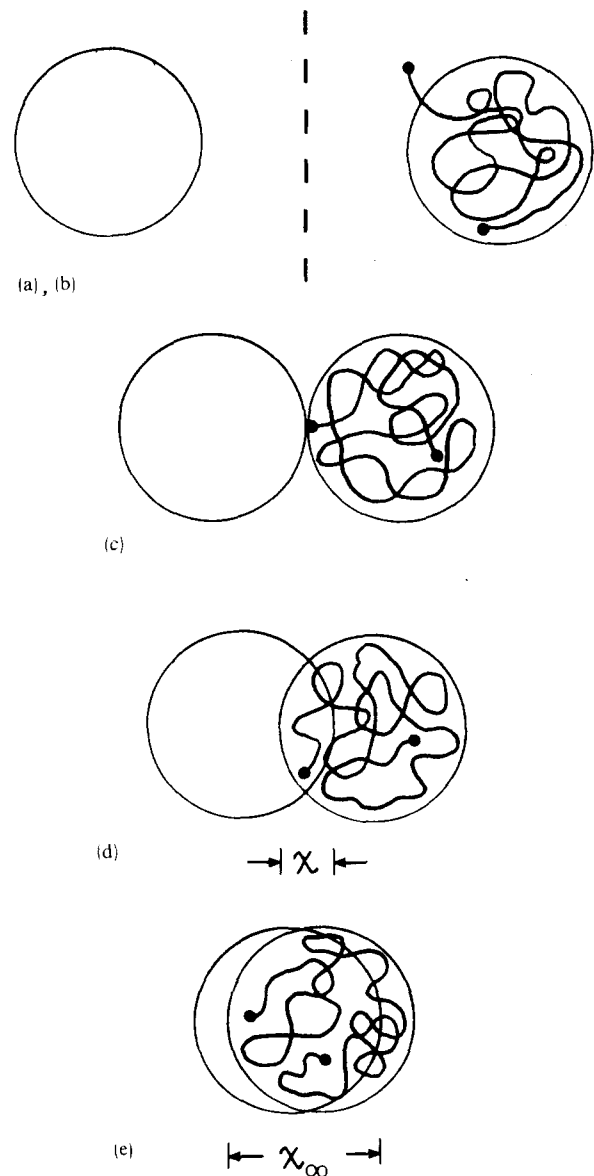

FIG. 2. Schematic diagram showing two random-coil chains on opposite crack surfaces during the five stages of crack healing (a) rearrangement, (b) surface approach, (c) wetting, (d) diffusion to a distance χ, and (e) diffusion to an equilibrium distance χ_∞ and randomization. Only one chain is shown for clarity. The dashed line represents the original crack plane.

theory with macroscopic importance. From our previous work with crack healing problems, we determined five stages of healing[8-15] which influence mechanical and spectroscopic measurements. They are as follows: (a) surface rearrangement, (b) surface approach, (c) wetting, (d) diffusion, and (e) randomization.

These stages of healing are shown schematically in Fig. 2 for chains of random walk character on opposite surfaces of a crack. The physical significance of each stage has been discussed in detail.[8-15] The relations for the stress transmitted across the crack plane, as measured by the fracture stress σ, are as follows:

Steps (a) and (b)

$$\sigma \geqslant 0, \tag{7}$$

where $\sigma = 0$ for large separation distances between molecules, and $\sigma > 0$ for the case of finite nonbonded interactions or possible interconnecting chain segments or fibrils.

Step (c)

$$\sigma = \sigma_0, \tag{8}$$

where σ_0 is the stress due to wetting or surface attraction.

Step (d)

$$\sigma = \sigma_0 + \sigma_d, \tag{9}$$

where σ_d is the stress due to random coil chains diffusing to an interpenetration distance χ normal to the interface.

Step (e)

$$\sigma = \sigma_\infty, \tag{10}$$

where σ_∞ is the fracture strength of the virgin material at the equilibrium interpenetration distance χ_∞.

The wetting and diffusion stages will determine the mechanical property development via the intrinsic healing function (to be discussed later).

B. Macro-micro correlation for healing

Consider a domain X in a crack interface or plane parallel to the interface in a material in which healing is occurring, as in Fig. 3. The set of all X defines the topology of the interface. In X the possibility arises that all stages of crack healing can exist simultaneously for different molecular pairs shown in Fig. 2. Therefore, the mechanical properties for X will be the sum of wetting and diffusion processes initiated at different times. This problem is conveniently resolved by defining an intrinsic healing function $R_h(t)$ for wetting and diffusion, and a wetting distribution function $\phi(X,t)$, such that the macroscopic recovery R, as defined by Eq.(1), is represented by the convolution process

$$R = \int_{\tau = -\infty}^{\tau = t} R_h(t - \tau) \frac{d\phi(\tau,X)}{d\tau} d\tau, \tag{11}$$

in which τ is the running variable on the time axis.

The lower integration limit $\tau = -\infty$ has particular significance for some $\phi(t,X)$. In many cases, partial disentanglement will have occurred, e. g., as in Fig. 2(d), which represents an incipient void. Therefore, its healing time in terms of $R_h(t)$ began at some $t < 0$ relative to a void with free or wetted surfaces Figs. 2(a), (b), and (c). This concept permits the treatment of damage due to disentanglement for
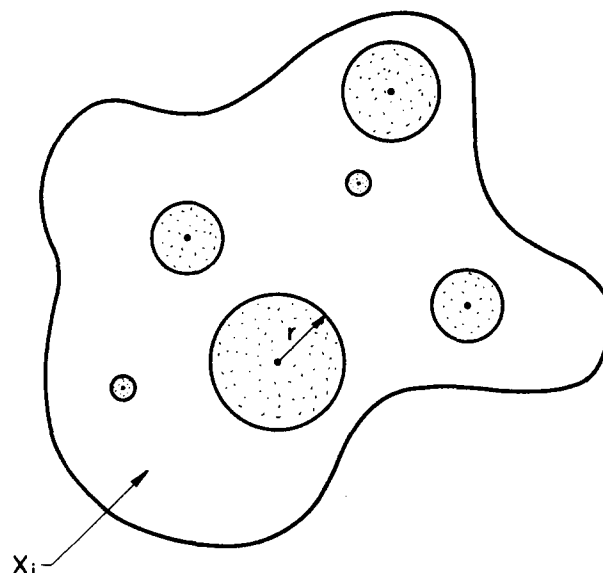

FIG. 3. Domain X_i in the interface of contacted crack surfaces is shown. The circular areas represent propagating wetted pools of radius r nucleated at various times τ.

materials which exhibit no cracks or voids due to mechanical work.

The line and point modes of healing can now be readily stated in terms of the wetting distribution function $\phi(t,X)$.

1. Line mode

Healing processes are equivalent in all domains of the interface or plane, thus

$$\phi(t,X_i) = \phi(t,X_j) \tag{12}$$

for all X_i.

2. Point mode

$$\phi(t,X_i) \neq \phi(t,X_j) \tag{13}$$

for some X_i, X_j.

Wetting distribution functions for point mode and mixed mode healing can be readily formulated as boundary value problems, or derived based on observation, particularly for the case of crack tip retreat.

The solution for many healing problems as represented by Eq. (11) can be determined if we know the intrinsic healing function $R_h(t)$ and the wetting distribution function $\phi(X,t)$. These functions are evaluated in the next section.

C. Wetting distribution function $\phi(X,t)$

Point mode healing in polymers is rare as a naturally occurring process,[3] but can be induced by controlling the local crack surface approach, e. g., while unloading a double cantilever beam specimen following crack advance. Such problems can be formulated for each individual material and test configuration, and will not be treated further here. We are primarily concerned with line mode healing for cracks, crazes, and voids in which healing processes occur uniformly in each X domain over the entire interface or representative plane in the material.

Our approach to the wetting function problem is a simple phenomenological one in which we consider wetting to proceed in a domain X by nucleation of wetting between chains on adjoining surfaces and propagation of wetted areas over the entire domain and interface. The wetted "pools" will propagate until they impinge with other pools and coalesce. This problem in two dimensions is analogous to the three-dimensional problem of nucleation and growth of spherulites or particles of known geometry as studied by Avrami[18] and Johnson and Mehl.[19]

As shown in Fig. 3, we let the wetted pools of area a be circular with radius r before impingement or coalescence, and consider nucleation $N(\tau)$ and radial growth $r(\tau)$ of wetted areas in the X domain. Before impingement, the total fractional wetted area $\phi'(t)$ is determined by

$$\phi'(t) = \frac{1}{A} \int_{-\infty}^{t} a(t-\tau)\dot{N}(\tau)d\tau, \tag{14}$$

where A is the total interfacial area in the X domain.

Correcting for impingement,[18] the wetting distribution function in X is obtained as

$$\phi(t) = 1 - e^{-\phi'(t)}. \tag{15}$$

The wetted area at time t of a single pool nucleated at time τ is

$$a(t-\tau) = \pi[r(t-\tau)]^2. \tag{16}$$

For linear radial propagation of wetted areas, we have

$$r(t) = k_s t, \tag{17}$$

where k_s is a spreading constant. For radial propagation by diffusion control we have

$$r(t) = (k_d t)^{1/2}, \tag{18}$$

where k_d is a constant.

Nucleation will be considered for two cases only; instantaneous nucleation, where

$$\dot{N}(t) = \delta(t), \tag{19}$$

in which $\delta(t)$ is the Dirac delta function, and for homogeneous nucleation, where

$$\dot{N}(t) = k_n U(t), \tag{20}$$

where $U(t)$ is a step function and k_n is a constant.

With Eqs.(16)–(20), a general set of solutions to Eq.(15) is obtained of the form

$$\phi(t) = 1 - e^{-kt^m}, \tag{21}$$

in which k and m are constants. The values for k and m are listed in Table I for various combinations of growth and nucleation behavior. It is reasonable to expect that the constants k_s, k_d, and k_n will be temperature and pressure dependent. We will consider three simple cases of wetting behavior.

(i) Instant wetting. A useful case to consider is when the two surfaces wet instantaneously and completely at $t = 0$. In this case, $k_s \to \infty$, $\dot{N}(t) = \delta(t)$ and we obtain

$$\frac{d\phi(t)}{dt} = \delta(t), \tag{22}$$

TABLE I. Wetting function constants.

Growth $r(t)$	Nucleation $N(t)$	k	m
$k_s t$	$\delta(t)$	πk_s^2	2
$k_s t$	$U(t)$	$\pi k_s^2/2$	3
$k_d t^{1/2}$	$\delta(t)$	πk_d	1
$k_d t^{1/2}$	$U(t)$	$\pi k_d/2$	2

(ii) Constant rate wetting. Another useful simple case is that of constant rate wetting before impingement and coalescence of wetted areas, such that $r = (k_d t)^{1/2}$, $\dot{N}(t) = \delta(t)$, and therefore

$$\frac{d\phi(t)}{dt} = k_d U(t), \tag{23}$$

(iii) Gaussian wetting. An important wetting distribution function for voids and incipient voids is that of a Gaussian distribution, where

$$\frac{d\phi(t)}{dt} = k_1 \exp[-k_2(t-t_0)^2], \tag{24}$$

in which k_1 and k_2 are constants, and t_0 is the time (positive or negative) for which the distribution has a maximum value. Equation (24) is not necessarily derivable from Eqs.(14)–(21).

Those equations are necessary to describe healing phenomena in polymers with different types of damage, e. g., incipient voids (partial disentanglement), voids, crazes, and cracks. With a suitable choice of $\phi(t)$, the crack healing problem is solved if the intrinsic healing function R_h is known.

D. The intrinsic healing function $R_h(t)$

The intrinsic healing function $R_h(t)$, used in Eq. (11), can be derived from an energy or stress consideration of mechanical property recovery during wetting and diffusion. This amounts to the choice of an energy or stress microfracture criterion. We will pursue this analysis using stress and later indicate parallel results derived from an energy approach. As in Eq.(9), we assume that the stress contribution from interpenetrating chains is the sum of a wetting component σ_0 and a diffusion component σ_d. The wetting component is obtained at the moment of contact of chains and the time dependence is thus controlled by self-diffusion of interpenetrating chains. Self-diffusion of random coil chains in the bulk can be treated by a reptation model of a chain confined to a tube, as discussed by de Gennes[20] and Edwards.[21] Useful discussion of this model can be found in papers by Klein[22] and DiMarzio,[23] and more recently, by Edwards.[24] In this model, shown in Fig. 4, a single chain of contour length L diffuses in a tube which represents the topological constraints on its motion imposed by the other chains in the bulk. In a time t_r, the curvilinear distance l travelled by the chain is given by the Einstein relation for a one-dimensional random walk in the tube as

$$\langle l^2 \rangle = 2D_c t_r, \tag{25}$$

where D_c is the curvilinear or reptation diffusion coefficient. D_c depends on molecular weight M as[20]
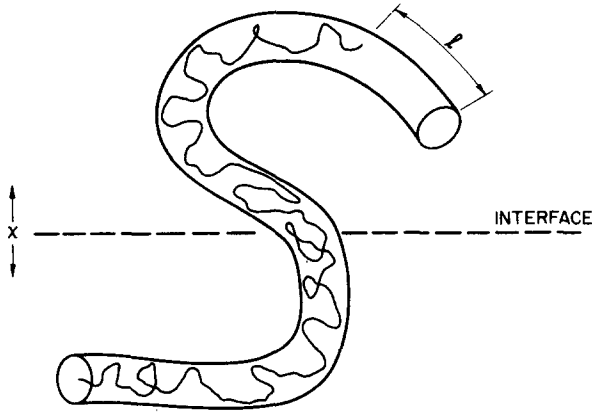
$$D_c \sim 1/M \tag{26}$$

FIG. 4. Reptation model for healing is shown as a random walk chain diffusing in a tube. The dashed line represents the crack interface which is normal to the interpenetration direction.

and temperature

$$D_c \sim T e^{-Q_d/kT}, \tag{27}$$

where Q_d is the activation energy for diffusion. The temperature dependence of D_c could also be expressed in other forms, including a WLF[29] approach by Williams, Landel, and Ferry, but the exact form here is not critical to the healing analysis. The hydrostatic pressure dependence of D_c is given to a first approximation by

$$\left(\frac{\partial \ln D_c}{\partial P} \right)_T = - \frac{\Delta V}{kT}, \tag{28}$$

where ΔV is the activation volume for segmental motion in the tube. Thus, Eq. (28) implies that D_c decreases with increasing P, which is a very important consideration for healing, welding, and melt processing of powder and pellet resin.

The tube contour represents another random walk with respect to the interpenetration distance χ, and therefore we have

$$\langle \chi^2 \rangle \sim \langle l^2 \rangle^{1/2}. \tag{29}$$

Thus, by virtue of the tube constraints which are presumed fixed for $\langle l^2 \rangle \simeq L^2$, the chain diffuses via a double random walk process, and from Eqs. (25) and (29), we obtain the important relationship

$$\langle \chi^2 \rangle^{1/2} = \alpha (2 D_c t_r)^{1/4} \tag{30a}$$

or

$$\chi \sim t_r^{1/4} \tag{30b}$$

for $t_r \leqslant t_\infty$, where t_∞ is the time to diffuse to the maximum interpenetration distance χ_∞ and α is a constant.

Equation (30) implies that the monomer diffusion proceeds as $\chi \sim t^{1/4}$ for distance of the order of χ_∞. At long times and long distances, $\chi \sim t^{1/2}$. The transition from $t^{1/4}$ to $t^{1/2}$ at $t \gg t_\infty$ is presently being evaluated.[25]

Having obtained $\chi \sim t^{1/4}$, we need to relate the mechanical properties σ, ϵ, E, and Y to χ to obtain their time dependence during healing. We assume that the mechanical

properties are related to the topological constraints experienced by each chain in the bulk. The constraints in the tube model represent the other chains' interactions with a chain in the tube and are expected to be of different character at individual points along the tube. For example, some chains will "touch" the tube chain while others form looped entanglements with a greater ability to restrict local motion of the chain in the tube and offer more resistance to mechanical deformation and flow. In this analysis, we consider the average effect of all the constraints along the tube on the mechanical properties of the chain. The number of constraints per chain, n_c, is simply

$$n_c = N/g, \tag{31}$$

where N is the degree of polymerization of the chain in the tube, and g is the average number of segments between constraints on the chain along the length of the tube.[22] The total number of constraints per unit volume of the virgin bulk material, n_0, is determined by the number of chains per unit volume multiplied by n_c as

$$n_0 = \left(\frac{\rho N_a}{N M_0} \right) \frac{N}{jg} = \frac{\rho N_a}{M_0 jg}, \tag{32}$$

where ρ is the bulk density, N_a is Avogadro's number, M_0 is the monomer molecular weight, and j is the number of chains involved in the average constraint, such that typically, $j = 2$ for an entanglement-type constraint. Thus, the number of constraints per unit volume is essentially independent of molecular weight, unless one could show that the spacing parameter g depends on M. Also, we can assume that the n_0 constraints are distributed uniformly in the bulk. Next, consider chains self diffusing across the interface to an interpenetration depth χ. The number of new constraints, n, generated by the chains diffusing across unit area A of interface will be linearly proportional to χ, i. e.,

$$n = n_0 \chi, \tag{33}$$

which means that n is the number of constraints in the interpenetration volume χA.

We now make an assumption which is intuitive rather than proven; i. e., that the stress σ_d is linearly proportional to the n constraints, as

$$\sigma_d = qn, \tag{34}$$

where q is a constant and from Eq. (33),

$$\sigma_d = q n_0 \chi \tag{35}$$

for $\chi \leqslant \chi_\infty$.

Equation (35) implies that the stress σ_d depends on the extent to which the chains are interpenetrated in each other, and thus the fracture stress is related to the interpenetration volume.

A modification to Eq. (35) would involve some critical interpenetration depth $\chi_c < \chi_\infty$, beyond which σ_d would not increase. This concept is implied in crack healing studies of Jud et al.[16] and has serious implications on mechanical properties versus molecular weight to be discussed later.

The time dependence of σ_d is obtained from Eqs. (30) and (35) as

$$\sigma_d = K t_r^{1/4}, \tag{36}$$

where

$$K = qn_0(2D_c)^{1/4}, \tag{37}$$

in which D_c is temperature, pressure, and molecular weight dependent, and n_0 is described by Eq. (32).

We now consider the diffusion initiation problem which is controlled by the surface rearrangement step. When a crack surface is created, chain ends are immediately available on the surface to initiate reptation following the wetting stage. However, if the surfaces associated with the domain X are not brought into contact immediately after fracture, these chain ends may diffuse into the bulk or undergo chemical reactions and surface rearrangement. Consequently, their diffusion across the interface at some later healing time would then be delayed or prevented. This problem can be resolved by designing a diffusion initiation function $\psi(t)$ such that σ_d is obtained as

$$\sigma_d = Kt^{1/4} \star \dot{\psi}(t), \tag{38}$$

where the star implies convolution. When all the necessary chain ends are available for immediate reptation across the interface (no surface rearrangement), then $\dot{\psi}(t) = \delta(t)$, and

$$\sigma_d = Kt^{1/4}. \tag{39}$$

When there is continuous initiation of diffusion at a constant rate

$$\dot{\psi}(t) = zU(t), \tag{40}$$

where z is a constant, and thus

$$\sigma_d = (4z/5)Kt^{5/4}. \tag{41}$$

When there is delayed but instantaneous diffusion at some time ζ

$$\dot{\psi}(t) = \delta(\zeta) \tag{42}$$

and

$$\sigma_d = K(t - \zeta)^{1/4}, \tag{43}$$

where ζ is a "delay" constant and $t \geqslant \zeta$.

The diffusion initiation problem solution was prompted by recent discussions with Tirrell[26] and is dealt with in considerable detail in a recent paper by Prager and Tirrell[27] in which they also consider a Gaussian distribution of chain ends near the surface.

The intrinsic healing expression for stress is thus obtained from Eqs.(9) and (37) as

$$\sigma = \sigma_0 + Kt^{1/4} \star \dot{\psi}(t), \tag{44}$$

which when divided by σ_∞ gives the intrinsic healing function

$$R_h(\sigma,t) = R_0 + \frac{Kt^{1/4}}{\sigma_\infty} \star \dot{\psi}(t), \tag{45}$$

where $R_0 = \sigma_0/\sigma_\infty$ is the wetting component.

The general healing expression for fracture stress in the case of line mode healing is obtained using Eq.(11) as

$$R(\sigma,t) = \left[R_0 + \left(\frac{K}{\sigma_\infty} t^{1/4} \star \dot{\psi}(t) \right) \right] \star \dot{\phi}(t). \tag{46}$$

The healing function for energy, $R(E,t)$ can be derived by assuming that the fracture energy E is related to the fracture stress σ via the linear elastic fracture mechanics relation

$$E = \tfrac{1}{2}\sigma\epsilon = \sigma^2/2Y, \tag{47}$$

where ϵ is the strain at fracture and Y is the tensile modulus. The intrinsic energy expression is obtained from Eq.(44), as

$$E = \frac{1}{2Y} [\sigma_0^2 + (2\sigma_0 Kt^{1/4} + K^2 t^{1/2}) \star \dot{\psi}(t)]. \tag{48}$$

Dividing by E_∞ and combining with Eq.(11), we obtain

$$R(E,t) = [R_0 + (K't^{1/4} + Gt^{1/2}) \star \dot{\psi}(t)] \star \dot{\phi}(t), \tag{49}$$

where

$$R_0 = \sigma_0^2/2YE_\infty = E_0/E_\infty, \tag{50}$$

$$K' = \sigma_0 K/YE_\infty, \tag{51}$$

and

$$G = K^2/2YE_\infty. \tag{52}$$

Had we chosen an energy criterion for the wetting and diffusion stages in Eq.(9), i. e., $E = E_0 + E_d$, we would obtain

$$R(E,t) = \{R_0 + [Gt^{1/2} \star \dot{\psi}(t)]\} \star \dot{\phi}(t), \tag{53}$$

which is similar to Eq.(49), except that $K' = 0$.

V. APPLICATIONS OF HEALING THEORY

The healing theory developed in the last section has application to cracks, crazes, voids, and incipient voids, but it is also useful for inferring properties of bulk polymers without cracks and has extensive application to systems for which surface-surface contact and fusion are important, for example, processing of powder and pellet resin and welding. In the following section, we use the healing theory to derive many predictions on mechanical properties during healing and provide experimental support for several of the predictions. We will first examine mechanical properties for the condition $\chi < \chi_\infty$, which will be called nonequilibrium properties. We will then examine equilibrium properties at $\chi = \chi_\infty$, and finally investigate the effect of T, P, and M on the time t_∞ to achieve χ_∞.

A. Strength at $\chi < \chi_\infty$
1. Instant wetting

Instant wetting, $\dot{\phi}(t) = \delta(t)$, involves (i) complete molecular contact at all possible wetting sites in each X domain of the crack interface, (ii) instantaneous optical disappearance of the crack interface, and (iii) immediate attainment of R_0, σ_0, or E_0. This may be possible for $T_h \gg T_g$, e. g., in polymer melts, elastomers at room temperature, and in cracks with very small and smooth surface areas. Assuming $\dot{\psi}(t) = \delta(t)$, we obtain from Eq. (46),

$$R(\sigma,t) = R_0 + Kt^{1/4}/\sigma_\infty. \tag{54}$$

This relation was investigated by a double cantilever beam fracture experiment with lightly crosslinked hydroxy-terminated polybutadiene at room temperature. Figure 5 shows a log-log plot of $R-R_0$ vs t for this crack healing experiment and a slope of 1/4 was obtained with excellent reproducibility. Other aspects and calculations based on this double cantilever beam experiment are discussed elsewhere.[13] In recent crack healing experiments with compact tension sam-
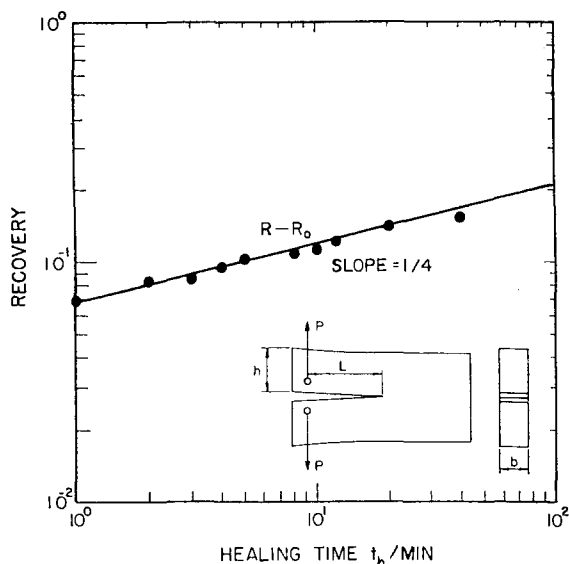
FIG. 5. Log of the recovery of the fracture load minus the wetting component $R - R_0$ is plotted vs the log of healing time for a double cantilever beam fracture healing experiment. The material used was lightly cross-linked polybutadiene at $T = 20$ °C.

ples of PMMA, Jud, Kausch, and Williams[16] obtained $\sigma = Kt^{1/4}$ for healing temperatures in the range 5–20 °C above T_g. They assumed that $\sigma_0 \simeq 0$ and that instant wetting occurred at these temperatures. In similar experiments, Tirrell[26] did not observe instant wetting for PMMA. However, his samples were twice as thick as those of Jud *et al.* Interesting differences in theoretical approach to crack healing exist between ourselves and these investigators.

Equation (54) should also be applicable to processing of powder or pellet resin by compression molding, such that the strength of the material in uniaxial tension would depend on the one-fourth power of the processing time, with a slope dependent on T, P, and M.

2. Constant rate wetting

When Eq. (23) is applicable for constant rate wetting and $\dot{\psi}(t) = \delta(t)$, we obtain from Eq. (46),

$$R(\sigma,t) = R_0 k_d t + 4k_d Kt^{5/4}/5\sigma_\infty. \tag{55}$$

Thus, before impingement of wetted areas occurs, the fracture stress will increase with an approximately linear dependence on t which will be a mixture of t^1 and $t^{5/4}$. However, if diffusion is small $(K \simeq 0)$ during the wetting stage, then

$$\sigma \sim t. \tag{56}$$

This could occur for very high molecular weight materials since $K \sim M^{-1/4}$.

Our preliminary studies of the fracture stress of compression molded ultrahigh molecular weight polyethylene powder $M \simeq 10^7$ indicated that Eq. (56) was applicable. When the samples were investigated by polarized light microscopy after different processing times, the gradual wetting between the powder particles was evident. Considerable improvement of the mechanical properties of this material could be achieved if interpenetration of chains between pow-

der particles could be promoted. However, this may be difficult at short processing times due to the very low reptation diffusion coefficient of the chains. For compaction and fusion of such materials, a modification to the wetting distribution function was suggested by experiment as

$$\phi(t) = \phi_0 + (1 - \phi_0)(1 - e^{-kt^m}), \tag{57}$$

where ϕ_0 is the instantaneous fractional gain of wetted area upon application of P and T in the mold at $t = 0$.

The magnitude of σ_0 and R_0 for wetting will depend on the topology of the interface and mode of fracture, such that rougher fracture surfaces will create larger R_0 values. These values will also be considerably larger than those implied from the equilibrium surface tension values determined from contact angle studies.

B. Fracture energy at $\chi < \chi_\infty$
1. Instant wetting

For instant wetting with $\dot{\psi}(t) = \delta(t)$ we expect that

$$R(E,t) = R_0 + K't^{1/4} + Gt^{1/2}, \tag{58}$$

provided that microscopic fracture is determined by a stress rather than an energy fracture criterion. Equation (58) was found to describe the fracture energy in the double cantilever beam experiment shown in Fig. 5, such that a log-log plot of $R - R_0$ vs t has a slope intermediate to 1/4 and 1/2. For the case where an energy criterion would be more suited than Eq. (9), we would obtain

$$R(E,t) = R_0 + Gt^{1/2}. \tag{59}$$

If $E_\infty \gg E_0$, then $R(E,t) \sim t^{1/2}$, regardless of whether a stress or energy microscopic fracture criterion is used.

2. Constant rate wetting

When $\dot{\psi}(t)$ is instantaneous and $\dot{\phi}(t) = k_d U(t)$, we obtain from Eq. (49)

$$R(E,t) = R_0 k_d t + \tfrac{4}{5}k_d K't^{5/4} + \tfrac{2}{3}k_d Gt^{3/2}. \tag{60}$$

If little diffusion occurs during the wetting stage, K' and $G' \simeq 0$, then again we have

$$R(E,t) \sim t. \tag{61}$$

The latter result was observed in the early stages of healing of Izod impact fracture in polystyrene.[13]

C. Fracture mechanics parameters K_{IC} and G_{IC}

The fracture toughness $K_{IC} \sim \sigma$ the fracture stress. Since $(\sigma - \sigma_0) \sim \chi \sim t^{1/4}$, in Eq. (44), then for instant wetting K_{IC} is given by

$$K_{IC} \sim t^{1/4} + C, \tag{62}$$

where C is a constant. Jud *et al.*[16] obtained $K_{IC} \sim t^{1/4}$ for PMMA single crack healing studies in which $C = 0$.

The critical strain energy release rate $G_{IC} \sim K_{IC}^2$. Therefore, from Eq. (62) we can have

$$G_{IC} \sim t^{1/2} + 2Ct^{1/4} + C^2, \tag{63}$$

and if C is small $G_{IC} \sim t^{1/2}$ as implied by the studies of Jud *et al.*[16] In our fracture studies with polybutadiene, the constant

C was not zero and the time dependence for K_{IC} and G_{IC} was as in Eqs. (62) and (63), respectively. These results are not inconsistent with those of Jud $et\ al.$, since in our case σ_0 was large compared to σ_∞, whereas with PMMA, σ_0 can be very small.

D. Elongation at $\chi < \chi_\infty$

If the elongation to break, ϵ, is proportional to the fracture stress, via $\sigma = Y\epsilon$, and Y is independent of χ, then we can have

$$\epsilon = \epsilon_0 + Jt^{1/4}, \tag{64}$$

where ϵ_0 is a wetting component of strain, and J is a constant dependent on P, T, and M.

E. Strength, elongation, and impact energy vs M at $\chi < \chi_\infty$

In this case, we consider how σ varies with M for some constant healing or processing time, $t_p < t_\infty$. Following the wetting stage, we have $(\sigma - \sigma_0) \sim \chi \sim (D_c t_p)^{1/4} \sim (t_p/M)^{1/4}$ from Eq. (26). Therefore

$$\sigma \sim M^{-1/4} + C, \tag{65}$$

where C is a constant. Similarly for ϵ,

$$\epsilon \sim M^{-1/4} + C. \tag{66}$$

Thus, with increasing M at constant healing time less than the equilibrium interpenetration time t_∞, we expect a decrease in both σ and ϵ. This is due to the decreased mobility of the chains with increasing M and affects the healing process via $D_c \sim M^{-1}$. This result was implied in recent healing studies of polystyrene (PS) pellets during compression molding,[14] and is discussed later with regard to Fig. 6.

If $E \sim \sigma^2/Y$, we expect for $\chi < \chi_\infty$ at constant t, that

$$E \sim M^{-1/2} + C. \tag{67}$$

We do not yet have data to test this relationship.

F. Equilibrium properties at $\chi = \chi_\infty$

As $\chi \rightarrow \chi_\infty$, we converge on the optimal mechanical properties of the material, i. e., by letting $\chi = \chi_\infty$ in all previous relations containing χ. Since $\chi \sim M^{1/2}$, we now have a convenient method of evaluating the effect of M on mechanical properties. Also, the time t_∞ at which $\chi = \chi_\infty$ provides a method of determining the reptation diffusion coefficient D_C.

G. Strength vs M at $\chi = \chi_\infty$

The equilibrium interpenetration distance χ_∞ at $t \geqslant t_\infty$ is determined by (see Fig. 2) $\chi_\infty = D - d$, where D is the diameter of the spherical envelope enclosing a random coil chain and d is the average spacing between centers of two adjacent chain spheres. D is given by[11]

$$D = 1.31(NC_\infty)^{1/2}b, \tag{68}$$

where C_∞ is the characteristic ratio, N is the degree of polymerization, and b is the length of each repeat unit. The average spacing parameter d is determined by

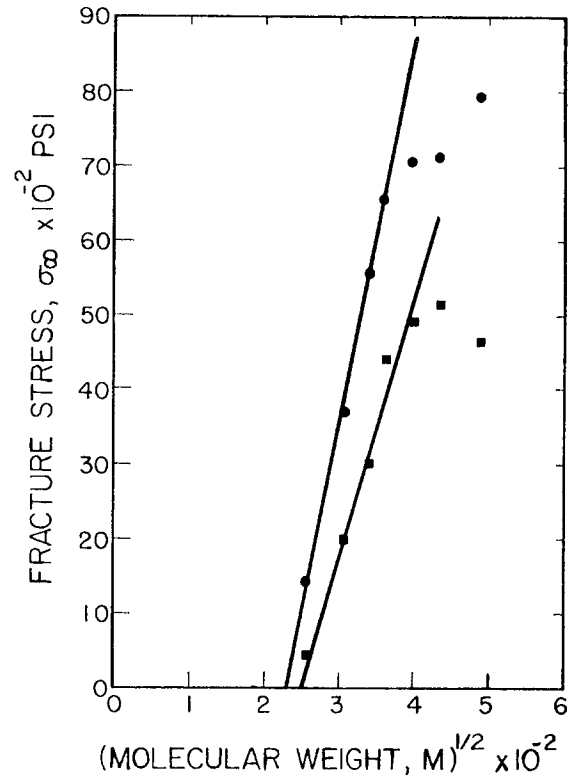$$d = (M/\rho N_a)^{1/3}. \tag{69}$$

FIG. 6. Tensile fracture stress is plotted vs square root of molecular weight for monodisperse atactic polystyrene prepared by injection (●) and compression molding (■).

Substituting Eqs. (68) and (69) in χ_∞, we obtain

$$\chi_\infty = aM^{1/2} - CM^{1/3}, \tag{70}$$

where a and C are constants, and typically, have values close to unity when χ_∞ is expressed in units of angstroms. For large M, the $M^{1/2}$ term dominates and we obtain $\chi_\infty \sim M^{1/2}$ as

$$\chi_\infty = 1.31b(C_\infty/M_0)^{1/2}M^{1/2}, \tag{71}$$

in which $M_0 = M/N$. At small M, χ_∞ deviates from the $M^{1/2}$ dependence. If the chain contour length $L = Nb$, then the constant α in Eq. (30a) is derived from Eq. (71) as $\alpha = 1.31(bC_\infty)^{1/2}$.

Since $(\sigma - \sigma_0) \sim \chi_\infty \sim M^{1/2}$, we obtain for strength

$$\sigma \sim M^{1/2} + C, \tag{72}$$

where C is a constant. This relation was investigated using the mechanical property vs M data for polystyrene (PS) obtained by McCormick $et\ al.$[28] Figure 6 shows a plot of fracture stress vs $M^{1/2}$ for anionic (approximately monodisperse) atactic PS tensile samples prepared by both injection molding and compresssion molding techniques. The injection molded samples were prepared using a melt (machine) temperature of 249 °C, a mold temperature of 52 °C and an injection pressure of 26 600 psi. The processing cycle time was not reported. Compression molded samples, $\frac{1}{8}$ in. thick, were prepared between heated platens in a hydraulic press using a temperature of 170 °C, a pressure of 40 000 lbs, and a molding time of 1 min for all materials. The latter time is of particular importance for determining D_c. We see in Fig. 6 that

for both processing methods, we have a range of M for which σ is linear with $M^{1/2}$, and at higher M, the data deviate from the linear relation. Also, for compression molding at constant time, σ decreases with increasing M beyond the linear region. For the injection molded case, the data are reasonably linear up to $M = 131\,000$ and can be described by

$$\sigma = 49.19(M^{1/2} - M_i^{1/2}) \tag{73}$$

using a least-squares fit with a correlation coefficient, $r^2 = 0.996$ ($1 =$ perfect linear fit), and the M intercept at $\sigma = 0$ was $M_i = 52\,700$.

The compression molded linear data region was described by

$$\sigma = 33.4(M^{1/2} - M_i^{1/2}), \tag{74}$$

where $M_i = 60\,270$ was obtained with a linear least-squares correlation fit parameter, $r^2 = 0.936$. We suggest that the linear region describes the equilibrium σ values for the processing time $t_p > t_\infty$, and that the nonlinear values at high M represent nonequilibrium σ values for $t_p < t_\infty$. The maximum value of σ in the linear region represents the case for which $t_p = t_\infty$ and occurs at $M = 159\,000$ and $t_p = 1$ min for the compression molded data. If the chain diffuses a curvilinear distance $L = Nb$ in a time t_∞ and $L^2 = 2D_c t_\infty$, then D_c is obtained as

$$D_c = (Nb)^2/2t_\infty. \tag{75}$$

Letting $N = 159\,000/104$ and $b = 2.55$ Å, we obtain $D_c = 1.27 \times 10^{-11}$ cm^2/sec at $T = 170$ °C and $P \simeq 2222$ psi. In Eq. (75) we used the planar zig-zag contour length for the chain which does not account for chain "slack" in the tube. This could be considered by using $N' = N/S$, where $S \geqslant 1$ and defines the ratio of the tube length to the extended chain contour length. However, this ratio is presently unknown.

The decrease in σ at high M shown in Fig. 6 for the compression molded data is predicted by Eq. (65), such that $(\sigma_1/\sigma_2) = (M_2/M_1)^{1/4}$. For example, if $t_p = t_\infty$ at $M_2^{1/2} = 398.7$ ($M_2 = 159\,000$) and $\sigma_2 = 4910$ psi, then in the nonlinear region at $M_1^{1/2} = 489.9$ ($M_1 = 240\,000$), we would expect that $\sigma_1 = 4910\,(159\,000/240\,000)^{1/4} = 4430$ psi. The calculated value for σ_1 compares with the observed value of $\sigma_1 = 4660$ psi. The dropoff in σ at high M is more pronounced for the compression molded data, perhaps because of the better control of the constant processing time compared with injection molding with two-stage heating at different times in melter and mold. The difference in slopes of σ vs $M^{1/2}$ for the compression and injection molded samples may be due to flow-induced anisotropy in the injection molded samples and other processing differences. Polydisperse PS behaves similarly to monodisperse PS.[14]

H. Elongation vs M at χ_∞

Since $\sigma \sim \epsilon$, we obtain

$$\epsilon \sim M^{1/2} + C. \tag{76}$$

For the σ data shown in Fig. 6, the ϵ data were described by[14]

$$\epsilon = 0.013\,(M^{1/2} - M_i^{1/2}), \tag{77}$$

where $M_i = 55\,483$ for the injection molded PS samples. For the compression molded samples, we obtained

$$\epsilon = 0.009\,(M^{1/2} - M_i^{1/2}), \tag{78}$$

where $M_i = 65\,153$. The prediction of $\epsilon \sim M^{-1/4}$ in Eq. (66) was also observed.

I. Impact energy vs M at χ_∞

We have $\sigma \sim \chi_\infty$, $E \sim \sigma^2/Y$, and $\chi \sim M^{1/2}$, thus we obtain

$$E \sim M + C. \tag{79}$$

Our recent studies[14] with PS using McCormick's data showed that for the same molecular weight range in which both σ and ϵ were linear with $M^{1/2}$, we obtained for impact energy of injection molded monodisperse PS,

$$E = 1.982 \times 10^{-4}M, \quad \text{ft-16/in}^3. \tag{80}$$

The latter relation was obtained with just three data points ($r^2 = 1.000$) and needs further investigation.

J. Fractured chains vs M at χ_∞

When a crack is propagating through a highly interpenetrated chain system, the number of ruptured bonds may depend on the number of chain spheres intersecting the fracture plane. In recent studies by Wool and Rockhill,[11] it was shown that the change in molecular weight M/M_f as a function of M during slicing of polydisperse PS could be described by

$$M/M_f = 1 + K_f(M^{1/2} - M_i^{1/2}), \tag{81}$$

where M_f is the molecular weight of the fractured slices, $M_i = 30\,000$, and K_f is a constant dependent on the fracture surface area and random coil parameters. This calculation involved the interpenetration volume $\chi_\infty A$ enclosing the fracture surface and since $\chi_\infty \sim M^{1/2}$, we have

$$M/M_f \sim M^{1/2} + C \tag{82}$$

in agreement with experiment.

In the next section we will consider the effect of T, P, and M on t_∞, the time to achieve complete interpenetration and complete healing.

K. Effect of temperature on t_∞

Temperature affects all stages of healing. T affects wetting by changing both the surface nucleation density of wetted areas and their propagation rate, which are important factors in the wetting distribution function $\phi(t)$. Thus at $T \simeq T_g$, we can have $\phi(t) = k_s U(t)$; and at $T \gg T_g$, $\phi(t) = \delta(t)$. The diffusion initiation function $\psi(t)$ will also be affected by temperature via surface rearrangement processes in a manner which remains to be determined more precisely. When both $\phi(t)$ and $\psi(t)$ are instantaneous, then $\chi_\infty \sim (D_c t_\infty)^{1/4}$, and thus

$$t_\infty \sim \exp(Q_d/kT). \tag{83}$$

The recovery $R(\sigma,t)$ as a function of temperature could be expressed by

$$R(\sigma,t) = R_0 + (K_0/\sigma_\infty)(a_T t)^{1/4}, \qquad (84)$$

where a_t is a time-temperature shift factor, and K_0 is the value of K at a reference temperature T_0. The shift factor can be described by an Arrhenius relation,

$$\log a_T = \frac{Q_d}{k}\left(\frac{1}{T_0} - \frac{1}{T}\right) \qquad (85)$$

or alternatively, by a WLF description.[29]

T also affects the equilibrium structure of the random walk chains determining χ. This is considered to be of secondary importance to the effect of T on wetting and diffusion. However, it may be an important consideration during rapid cooling to $T < T_g$, such that χ_∞ does not attain its equilibrium value and subsequently changes the strain energy function of the chains in the glass.[30]

As noted in many of our experimental studies of healing, temperature has a marked effect on the healing rate. However, caution should be exercised in extracting precise information on activation energies for diffusion, etc., since the results usually include contributions from both wetting and diffusion.

L. Effect of pressure on t_∞

From $\chi_\infty \sim (D_c t_\infty)^{1/4}$ and $D_c \sim \exp(-P)$, we obtain

$$t_\infty \sim \exp P. \qquad (86)$$

This relationship suggests that since the applied pressure increases the time necessary to achieve maximum interpenetration, that P should be decreased following the wetting stage. An initial high pressure to facilitate wetting which then relaxes to zero is recommended for processing and welding where surface contact and diffusion are important.

M. Effect of molecular weight on t_∞

We have $\chi_\infty \sim M^{1/2}$ and $\chi_\infty \sim (D_c t_\infty)^{1/4}$. Also $D_c \sim M^{-1}$. Therefore,

$$(t_\infty/M)^{1/4} \sim M^{1/2}, \qquad (87)$$

and thus

$$t_\infty \sim M^3. \qquad (88)$$

De Gennes[20] derived a similar relation for the "renewal" time of a chain in a tube.

In Fig. 6, the processing time t_1 for PS with $M_1 = 240\,000$, to achieve optimal properties is determined from

$$t_1 = t_2(M_1/M_2)^3, \qquad (89)$$

where $t_2 = 1$ min at $M_2 = 159\,000$, yielding $t_1 = 3.44$ min. Had the compression molding time been increased from 1 to 3.44 min, then the strength of the material with $M = 240\,000$ would have increased from its present value of 4660 to 8166 psi, as determined in Eq. (74).

In all of the above property predictions with M, we have not introduced any upper limit on properties with M. We developed a theory in terms of the number of constraints in the interpenetrated volume which scales with χ_∞ and hence $M^{1/2}$. This is analogous to the scaling relation for melt vis-

cosity $\eta \sim M^3$ (Ref. 20) which compares with the experimental result, $\eta \sim M^{3-4}$ for $M > M_c$, where M_c is the "critical entanglement" molecular weight. However, it is conceivable that an upper limit for χ_∞ exists; e. g., χ_c such that for all $\chi_\infty > \chi_c$, the mechanical properties do not change and become independent of molecular weight. We have not yet observed this effect in our studies, but it may have been observed in Kausch's crack healing studies.[31]

N. Stress relaxation and creep

The topological constraints controlling chain mobility in a tube during interpenetration are similar to those for the reverse step, i. e., disentanglement by separation of random walk chains. If we make the primitive assumption that the time dependence for the gain of n constraints is the same as the loss of n constraints, such that $\chi \sim t^{1/4}$, then for the creep compliance, $J(t)$, of viscoelastic polymers, we obtain

$$J(t) = J_0 t^{1/4},$$

where J_0 is constant.

The stress-relaxation modulus $G(t)$ for this same process is

$$G(t) = G_0 t^{-1/4},$$

where G_0 is a constant. The latter equation is often called the "inverse power law" description for $G(t) = Gt^{-n}$, where n is an experimental constant, and is assumed to be strictly empirical. However, many polymer materials, such as filled elastomers, carbon-black filled rubber, solid rocket propellant, and other lightly crosslinked amorphous polymers exhibit this behavior with $n \simeq 1/4$.[32]

Linear and nonlinear time-dependent properties, which are important for determining constitutive relations for viscoelastic polymers, are being further investigated by this theoretical approach and that of Doi.[33]

VI. SUMMARY

A theory of crack healing in polymers was presented with respect to the five stages of crack healing. The surface rearrangement stage effects the diffusion initiation function and topological features of the interface. The approach stage controls the mode of healing, i.e., point or line mode. The wetting stage controls the wetting distribution function. The diffusion stage is the most important stage controlling the development of mechanical properties during healing. The randomization stage involves complete loss of memory of the crack interface.

The extent of healing or recovery was determined as a convolution product of the wetting distribution function with an intrinsic healing function. The reptation model for a chain diffusing in a tube was found to be excellent in providing a molecular basis for the time dependence of the intrinsic healing function, $R_h(t)$ via $\chi \sim t^{1/4}$. The wetting distribution function $\phi(t)$ was formulated by a phenomenological approach in parallel with the Avrami analysis of crystallization such that nucleation and propagation of wetted areas in the crack interface was considered. The resulting expression for $R_h(t) * \dot{\phi}(t)$ provided a wide range of possible time dependences for healing based on the choice of $\phi(t)$ and the diffu-

TABLE II. Summary of theoretical relationships.

$X \sim t^{1/4}$	$(t \leqslant t_\infty)$
$\sigma, \epsilon, K_{IC}, \sim t^{1/4} + c$	$(t \leqslant t_\infty)$
$E, G_{IC}, \sim t^{1/2} + c$	$(t \leqslant t_\infty)$
$\sigma, \epsilon, K_{IC} \sim M^{1/2} + c$	$(t \geqslant t_\infty)$
$E, G_{IC} \sim M + c$	$(t \geqslant t_\infty)$
$\sigma, \epsilon, K_{IC} \sim M^{-1/4}$	$(\text{const. } t < t_\infty)$
$E, G_{IC} \sim M^{-1/2}$	$(\text{const. } t < t_\infty)$
$t_\infty \sim M^3$	
$t_\infty \sim \exp P$	
$t_\infty \sim \exp 1/T$	
$M/M_f \sim M^{1/2} + c$	(chain scission)
$G(t) = G_0 t^{-1/4}$	(inverse power law material)
$J(t) = J_0 t^{1/4}$	(power law material)

sion initiation function $\psi(t)$ in $R_h(t)$.

Relations for strength, elongation to break, impact energy, and fracture parameters were obtained as a function of time, molecular weight, temperature, pressure, and processing conditions. Most of the theoretical predictions are summarized in Table II. Many of these predictions were supported by experimental data for single crack healing and processing of pellet resin. We are continuing to analyze both craze and void healing data to determine a suitable choice of $\phi(t)$ for each healing system.

The crack healing theory developed in this paper provides a basis for understanding the concept of damage as well as healing in polymer materials, and permits a better understanding of mechanical properties. The majority of the theoretical predictions have been verified experimentally but several remain to be demonstrated. In particular, we are examining problems of chain self-diffusion at short and long distances for application to crack healing and polymer processing.

[1] R. P. Wool, Poly. Eng. Sci. **18**, 1057 (1978).
[2] R. P. Wool, ACS Org. Coat. Plast. Chem. **40**, 271 (1979).
[3] R. P. Wool, *Adhesion and Adsorption of Polymers*, edited by L-H Lee (Plenum, New York, 1980), Part A, pp. 341–362.
[4] R. P. Wool, "Network Fracture in Fibers and Films," Paper No. 21S, Proceedings of the 69th Annual Meeting of A. I. Ch. E., Chicago, 1976.
[5] R. P. Wool, M. I. Lohse, and T. J. Rowland, J. Polym. Sci. Lett. **17**, 385 (1979).
[6] K. M. O'Connor and R. P. Wool, J. Appl. Phys. **51**, 5075 (1980).
[7] K. M. O'Connor and R. P. Wool, J. Polm. Sci. Phys. Ed. (to be published).
[8] R. P. Wool and K. M. O'Connor, ACS Polym. Preprints **21**, 40 (1980).
[9] R. P. Wool and K. M. O'Connor, Poly. Eng. Sci. **21**, (in press).
[10] R. P. Wool and A. T. Rockhill, ACS Polym. Preprints **21**, 223 (1980).
[11] R. P. Wool and A. T. Rockhill, J. Macromol. Sci. Phys. **20**, No. 1, xxx (1981).
[12] R. P. Wool, "Crack Healing in Composites," ACS Polymer Preprints **22**, 207 (1981).
[13] R. P. Wool and K. M. O'Connor, J. Polym. Sci. Lett. **19** (1981).
[14] R. P. Wool, J. Polym. Sci. Phys. Ed. (to be published).
[15] R. P. Wool, "Material Damage in Polymers," Proceedings of NSF Workshop on A Continuum Mechanics Approach to Damage and Life Prediction, Kentucky, May 1980, pp. 28–35.
[16] K. Jud, H. H. Kausch, and J. G. Williams, J. Mater. Sci. **16**, 204 (1981).
[17] P. G. de Gennes, C. R. Acad. Sci. Paris, B **291**, 219 (1980).
[18] M. Avrami, J. Chem. Phys. **7**, 1103 (1939).
[19] W. A. Johnson and R. F. Mehl, Trans. AIME A **16**, 135 (1939).
[20] P. G. de Gennes, J. Chem. Phys. **55**, 572 (1971).
[21] S. F. Edwards, Proc. Phys. Soc. **92**, 9 (1967).
[22] J. Klein, Macromolecules **11**, 852 (1978).
[23] E. A. DiMarzio, C. M. Guttman, and J. D. Hoffman, Faraday Discussions **68**, (1979).
[24] S. F. Edwards, Polymer Preprints **22**, 182 (1981).
[25] Y. H. Kim, K. M. O'Connor, and R. P. Wool (paper in preparation).
[26] M. Tirrell (private communication).
[27] S. Prager and M. Tirrell (paper submitted for publication).
[28] H. W. McCormick, F. M. Brower, and L. Kim, J. Polym. Sci. **39**, 87 (1959).
[29] M. L. Williams, R. F. Landel, and J. D. Ferry, J. Amer. Chem. Soc. **77**, 3701 (1955).
[30] R. P. Wool and R. H. Boyd, J. Appl. Phys. **52**, 5116 (1980).
[31] H. H. Kausch (private communication).
[32] J. D. Ferry, *Viscoelastic Properties of Polymers*, 2nd edition (Wiley, New York, 1970).
[33] M. Doi, Polymer Preprints **22**, 100 (1981).